

## Article

# Deep Neural Network Model for Determination of Coal Cutting Resistance and Performance of Bucket-Wheel Excavator Based on the Environmental Properties and Excavation Parameters

Srdjan Kostić <sup>1,2,\*</sup> , Milan Stojković <sup>3</sup> , Velibor Ilić <sup>3</sup>  and Jelena Trivan <sup>4</sup><sup>1</sup> Jaroslav Černi Water Institute, Jaroslava Černog 80, 11226 Belgrade, Serbia<sup>2</sup> Faculty of Technical Sciences, University of Novi Sad, Trg Dositeja Obradovića 6, 21000 Novi Sad, Serbia<sup>3</sup> The Institute for Artificial Intelligence Research and Development of Serbia, Fruškogorska 1, 21000 Novi Sad, Serbia; milan.stojkovic@ivi.ac.rs (M.S.); velibor.ilic@ivi.ac.rs (V.I.)<sup>4</sup> Faculty of Mining, University of Banja Luka, Aleja Kozarskog Odreda 1, 79101 Prijedor, Bosnia and Herzegovina; jelena.trivan@rf.unibl.org

\* Correspondence: srdjan.kostic@jcerni.rs or srdjan.kostic@uns.ac.rs

**Abstract:** In the present paper, we develop a new model, based on the implementation of deep neural networks, for the estimation of a series of excavation parameters, depending on the main environmental and excavation properties. The developed model, with high statistical accuracy ( $R > 0.79$ ) and small RMSE ( $< 17\%$  of the actual output values), enables the simultaneous assessment of the following excavation parameters: effective capacity  $Q_{ef}$ , maximum current consumption  $I_{max}$ , maximum power consumption  $N_{max}$ , maximum force consumption  $P_{max}$ , maximum energy consumption  $E_{max}$ , and maximum linear and areal cutting resistance,  $K_{Lmax}$  and  $K_{Fmax}$ , respectively, based on the impact of the following environmental properties and excavation parameters: coal unit weight, coal compression strength, coal cohesion, friction angle, excavator movement angle in the left and right direction, slice height and thickness, and wheel velocity. The data analyzed in the present paper were previously collected from three neighboring open-pit coal mines in Serbia: Tamnava Western Field, Tamnava Eastern Field, and Field D. These mines have similar geological conditions and coal properties. Additionally, for each output factor, a complex analysis is provided on the impact of the examined input factors, by applying the multiple linear regression method. As far as we are aware, this is the first time such a comprehensive estimation model has been suggested for the operation of a bucket-wheel excavator in the Neogene coal basins. The deep neural network (DNN) model, trained over 300 epochs, shows an MSE range of 6.7–16.5% across various input factors, with distinct evaluations for  $I_{max}$  due to its unique values (4.8–12.5%).

**Keywords:** coal surface mining; bucket-wheel excavator; interactions; deep neural network

**Citation:** Kostić, S.; Stojković, M.; Ilić, V.; Trivan, J. Deep Neural Network Model for Determination of Coal Cutting Resistance and Performance of Bucket-Wheel Excavator Based on the Environmental Properties and Excavation Parameters. *Processes* **2023**, *11*, 3067. <https://doi.org/10.3390/pr11113067>

Academic Editors: Minghui Li and Xiting Long

Received: 18 September 2023

Revised: 18 October 2023

Accepted: 24 October 2023

Published: 26 October 2023



**Copyright:** © 2023 by the authors. Licensee MDPI, Basel, Switzerland. This article is an open access article distributed under the terms and conditions of the Creative Commons Attribution (CC BY) license (<https://creativecommons.org/licenses/by/4.0/>).

## 1. Introduction

For decades, coal exploitation has been representing the main energy source for most countries worldwide. According to Gordon [1], Poland, the United States, the USSR, the United Kingdom, and Germany were the top five global coal-producing countries from 1900 to 1984. In these countries, coal production was the backbone of the industry development, i.e., coal was the source that accounted for the highest share in electricity production in these and many other countries throughout the world. This reliance on coal as the major source of electricity production reached its peak in 1990. When the calls for more strict environmental protection increased, many countries started to abandon this energy source and turned to more “clean” sources, like wind power, solar power, and hydropower, as the so-called green sources of energy. Around 40% of electricity was produced by consuming coal in 1990, while this number declined to 30% in 2022 worldwide [2–4]. In Germany, for instance, this number is even more pronounced: electricity production

from coal declined from 60% to 30% from 1990 to 2022. Also, in Poland, more than 95% of electricity production came from coal in 1990, while this number dropped to 70% in 2022. Probably the best illustration of this coal abandonment process is the one in the United Kingdom [5]. In the UK, coal production peaked in 1913, when it was produced approximately 292 million tons of coal, while in 2019, it was 150 times lower. Moreover, deep-mine coal production was completely abandoned until 2019. The number of employees in the coal production sector dropped from 1.2 million in the 1920s to approximately 600 thousand in 2019. The use of coal also drastically changed. Earlier, coal was commonly used in industry, railways, gas production, and heating in homes, while today it is only used for electricity production. In the end, coal was the primary energy source for a long time: 1900's coal supplied more than 95% of the demand; in the 1950s, this number was still above 90%, while in 2019, coal supplied only 3% of the energy demand.

Although there is a strong will and commitment among the top developed countries in the world to increase the participation of these green energy sources in total energy production, the corresponding infrastructure is still underdeveloped, and, in many cases, it is more expensive than the continuation of the coal excavation process, using the existing infrastructure, even in the case when more strict environmental measures are applied. Adding to this the current crisis with the supplement of coal/oil/gas, one can conclude that for now (and at least in the near future) countries need to maintain the coal excavation process and, in such a way, preserve, more or less, a sort of energy independence. Today, ten countries, namely, China, the USA, India, Poland, South Africa, Indonesia, Australia, Germany, Russia, and Kazakhstan, have an annual coal production of more than 100 Mt, i.e., approximately 95% of the overall coal production in the world. Half of this world production comes from China, which is accounted as the country with the highest coal production [6]. In Serbia, surface coal mining still represents the dominant method of coal exploitation. Excavated coal is further processed at thermal power plants, which provide approximately 70% of total electricity production in Serbia [7].

Concerning the current importance of coal excavation and its possible negative effects on the environment, it is of paramount importance to plan and execute coal exploitation in the most optimized way, to perform the excavation as quickly as possible, which will secure the on-time electricity production, and keep the exposure of the environment to the by-products of coal exploitation at the minimum level. There have been several previous attempts to optimize the coal excavation process using the bucket-wheel excavator. A previous fatigue study conducted by Andras et al. [8] used a computer model of the boom of a bucket-wheel excavator developed in SolidWorks. Based on this model, they estimated the period to material failure to reduce the hazard to any form of surface mining activities or the work of any industrial machine. Jiang et al. [9] analyzed the resistance to cutting by invoking the discrete element method and experimental design. The results of their research indicate that the resistance to cutting would decrease as the grain size and cutting velocity increase. The results of their study also indicate that the increasing cohesion among particles can have a positive effect on the resistance to cutting by adding the cohesive force between particles, or it can reduce the resistance by lowering the particle volume fraction through the so-called "big aggregates effect". Popescu et al. [10] analyzed the reaction time of the excavator during the excavation process. In particular, they examined the response of an excavator boom exposed to non-stationary force, by using the virtual model of a boom. The results of their research indicate that wheel velocity and the number of buckets significantly affect the high and slowly varying forces generated during the coal excavation process. Sowala et al. [11] examined how the choice of excavation parameters at the open-pit lignite mine is affected by the maneuvering movements of the excavator when the stabilized front is cleared out of the coal overburden. The results of their research show that the length of maneuvering roads is a more significant factor than the floor height in the case of excavation with both variable vertical and horizontal divisions. Machniak and Koziol [12] analyzed the mining process of solid rocks using bucket-wheel excavators. They proposed a new method for estimating the workability of solid rocks, in the form of a complex relationship

of breaking by tractor rippers and rock compressive strength, velocity of seismic waves, rock density, and the workability classification according to Bulukbasi [13]. Che and Chen [14] provided a theoretical analysis of bucket-wheel excavator production. The results of their study emphasize the need for adequate adjustment of the speed of the bucket-wheel excavator. In fast excavation, a nonuniform distribution of material flow occurs, which further causes a decrease in capacity utilization leading eventually to an unreliable inference between structure and performance parameters. Additionally, the excessive rotary speed of the excavator body will cause an increase in the excavator power consumption, drive power, cost of extraction, and mechanical strength required. Regarding the use of artificial intelligence-based methods for the performance optimization of machines in general, Xiang et al. [15] used deep learning algorithms to enhance the performance of machine regeneration, by invoking deep neural networks, convolutional neural networks, and recurrent neural networks. Also, Xiang et al. [16] apply the same approach to the on-site training of mobile construction machines. Nevertheless, as far as we know, there have been no previous attempts to develop a suitable model for the optimization of the bucket-wheel excavator performance based on the deep neural network approach.

In our previous papers, we evaluated the overburden cutting resistance and energy consumption and suggested the method for the optimization of the coal overburden excavation, which also takes into account the geomechanical properties of the terrain and states of the excavator's teeth. In particular, we examine the impact of the overburden geomechanical properties on the excavation parameters (wheel velocity and current consumption) for two different states of excavator's teeth: new and worn-out teeth after a minimum of 250 h of work [17]. According to the results of this study, there are statistically significant two-factor interactions with the increasing influence of overburden friction angle and unit weight on excavator current consumption and wheel velocity. On the other side, overburden cohesion is generally inversely proportional to the examined parameters of the excavation process. In contrast to our previous research, here we examine the case of coal excavation, with the following input factors: (1) coal properties: unit weight, compressive strength, cohesion, and friction angle; and (2) excavation parameters: excavation direction, slice height and thickness, and wheel velocity. The effect of these input factors is examined for the following output parameters: excavator capacity, maximum current consumption, maximum power consumption, maximum force consumption, maximum energy consumption, and maximum linear and areal cutting resistance. The influence of each of the input factors on the chosen output factors is thoroughly examined, including the significant two-factor interactions. The dependence of each analyzed output factor on the examined input factors is represented in the form of an explicit mathematical model. As a result, we suggest a unique artificial intelligence-based model, which enables the reliable estimation of the output factors, based on the value of one or several chosen input variables.

## 2. Methodology and Data Analyzed

We analyze a dataset of 198 recordings made at different open-pit coal mines in Serbia: Tamnava Eastern Field, Tamnava Western Field, and Field D, which all belong to the Kolubara coal mine in Serbia (Figure 1).

Coal properties at all three locations are the same or similar (coal is of the same origin, and with similar petrological and geomechanical properties), so it was possible to examine the whole dataset as unique data.

The Kolubara coal basin consists of a productive Neogene series lying on a paleo-relief of Paleozoic crystalline shale and Mesozoic sediments breached by dacite-andesitic eruptions of Tertiary age [18]. The productive series of lignite is grouped in three thick layers and several thinner layers, located in the lower part of the series. Both the overlaying and underlying parts of the coal series are composed of the sediments of the upper Pontian age, except in the parts where erosion has carried away the overlaying part. Upper Pontian sediments in the basin are developed in the facies of clay, sandy, and silty clays and sands, which alternate in the vertical and lateral directions. These sediments are with the

predominant clay fraction in the eastern part of the basin and with the predominant sand fraction in the western part. The Quaternary formations lie over Pontian sediments with an erosional-tectonic or erosional discordance. Pleistocene silts with layers and lenses of lacustrine-terrace gravels and sands compose a larger part of the terrain, while Quaternary alluvial gravel–sand sediments compose the river valleys.

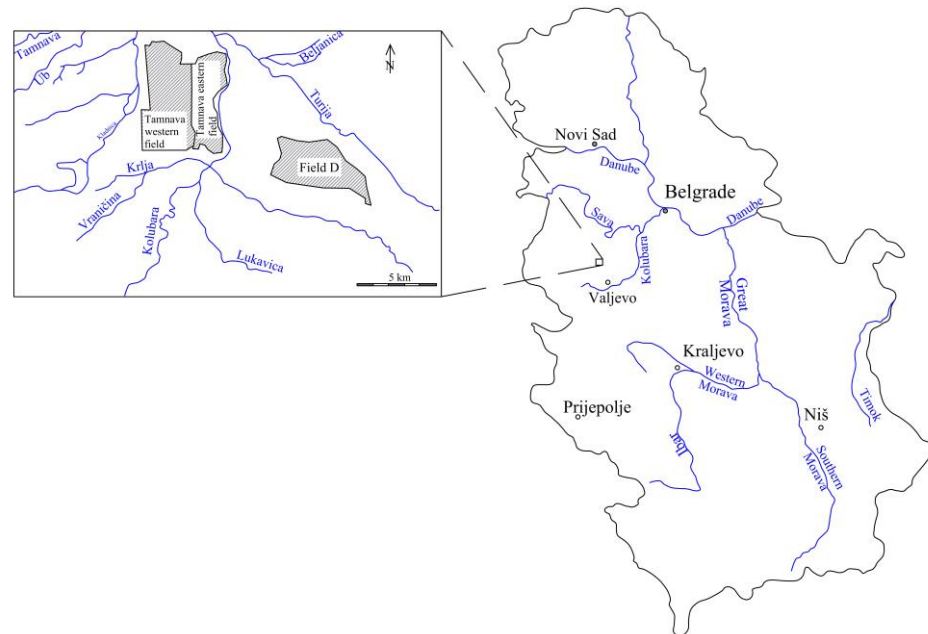


**Figure 1.** Locations of Tamnava Eastern Field, Tamnava Western Field, and Field D, from which data were collected and further analyzed.

At Field D, the main layer is excavated, while the sub-layer, recorded in the eastern part of the field, has no exploitable thickness [18]. The thickness of the main layer is 14–40 m and in the southeastern part of the field it lies on clays, while in the rest, the larger part, it lies on sands of different grain sizes. In the overlaying part, there are thick deposits of fine grain to silty sands and silty clays, which are covered by Quaternary clays (Figure 2).

At the Tamnava Eastern Field, the underlying layer of the coal seam is composed of 100 m thick sand (Figure 2). The main coal layer is above the sand, with a coal thickness of about 10–30 m. In the northwestern part of the terrain, this coal seam contains layers of 2–7 m thick sand. The overlaying layer is composed of silty clay with occurrences of lenses of fine-grained sands up to 28 m thick. The strong effect of erosion carried away part of the Pliocene sediments, so that the Kolubara alluvium rests partly on the Pliocene sediments and partly on coal. Alluvial gravels and sands with silt reach a thickness of up to 15 m [18].

At the Tamnava Western Field, the underlying layer is also made of fine-grain sand. The coal series has a complex composition: two thinner coal layers corresponding to the third coal layer (continuity not confirmed) were developed in the lower part, followed by the second 2–8 m thick coal layer and the first 10–20 m thick coal layer. Between the coal layers are fine-grain sands, very similar to the underlying sands. In the first coal layer, there are interlayers of clay, and rarely are there interlayers or lenses of sand. In the overlaying part of the first coal layer, there are silty clays and, to a lesser extent, silty quartz sands. In the southern part of the field, the Pliocene sediments are covered with lacustrine-terrace gravels. In the northeastern part, in the Kladnica River valley, the Pliocene sediments are covered by alluvial gravels, sands, and silts up to 10 m thick.

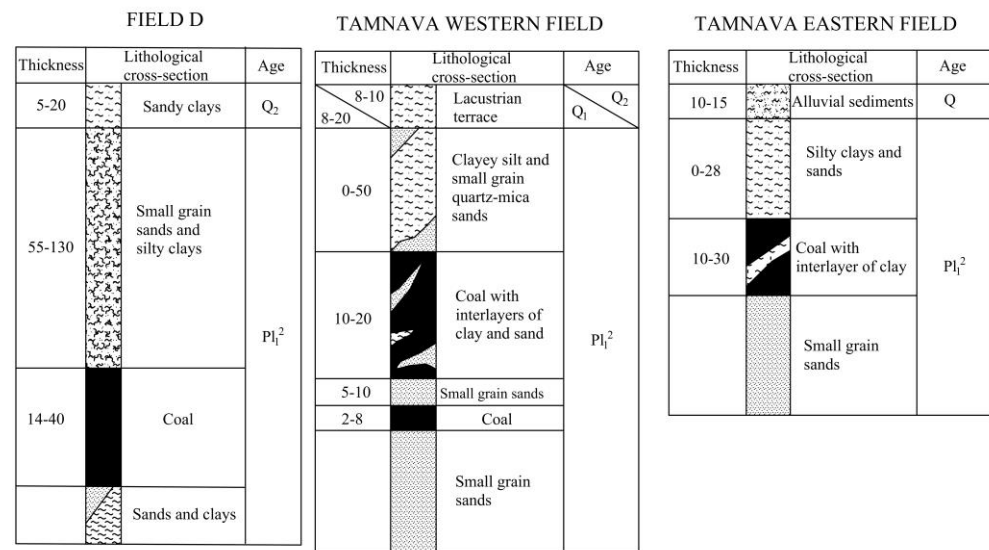


**Figure 2.** General lithological composition of open pits Field D, Tamnava Western Field, and Tamnava Eastern Field (according to [18]).

The main properties of the input and output data are presented in Table 1, according to [18].

Data were collected [18] for the case of coal excavation with bucket-wheel excavators of the same type, SchRs630, with the following main properties:

- Installed power for rotary wheel engine:  $2 \times 500$  kW (at Tamnava Western Field) and  $2 \times 375$  kW (at Tamnava Eastern Field and Field D)
- Bucket volume: 630 L
- Number of buckets: 20
- Number of buckets emptied: 162 per min
- Angular distance between buckets:  $18^\circ$
- Rotary wheel diameter: 10 m
- Length of rotary arrow: 35 m
- Wheel velocity: 4.24 m/s

All output factors, except  $K_{Lmax}$  and  $K_{Fmax}$ , were measured at the excavator.  $K_{Lmax}$  and  $K_{Fmax}$  were determined in laboratory conditions with the Orenstein and Koppel cut test. Coal unit weight, compressive strength, cohesion, and friction angle were determined in the laboratory, while  $\varphi_L$ ,  $\varphi_D$ ,  $h$ ,  $s$ , and  $V_b$  were set on the excavator.

The effect of the chosen input (controlling) factors on the output factors was examined in two phases. In the first phase, we invoke the multiple linear regression method and derive separate mathematical expressions for the dependence of each singular output factor on the examined controlling factors. The results of these analyses are evaluated using basic statistical parameters and the ANOVA test. In the second phase of the research, we develop a single model based on artificial neural networks, which enables the estimation of multiple output factors based on the significant impact of the controlling parameters.

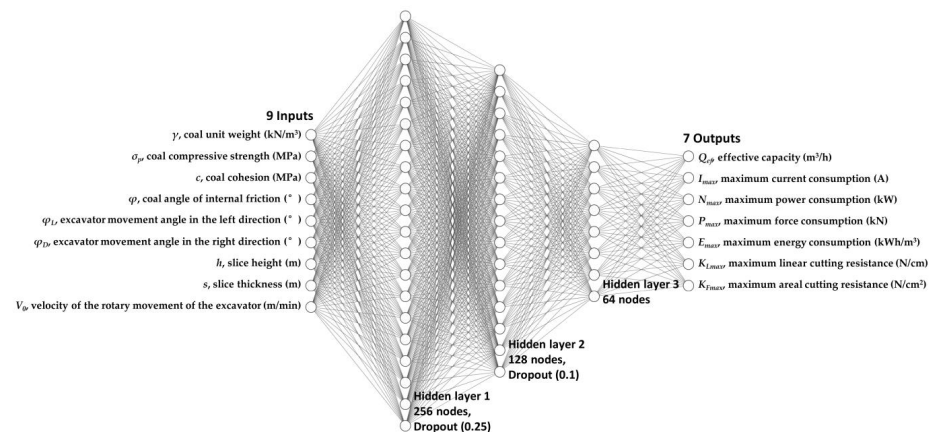
Regarding the development of the deep neural network (DNN) model, the dataset consists of 198 measurements of 16 variables, of which 9 variables represent the input to the model, i.e., the parameters based on which the prediction is made, as shown in Table 1. Given that the dataset consists of variables expressed in different units, with each variable moving in its range, before training the model, it is necessary to determine the minimum and maximum values for each variable, and then, based on these values, the values are normalized to the range [0,1]. Before training the model from the data, 20% of the total dataset is set aside for testing. The remaining dataset is then split into 80% data used to train the network and 20% data to be used for validation during training.

**Table 1.** Overview of the examined input and output data.

Output Factors	Range of Values
$Q_{ef}$ , effective capacity ( $m^3/h$ )	239.3–1782
$I_{max}$ , maximum current consumption (A)	25–1335
$N_{max}$ , maximum power consumption (kW)	314.8–755.5
$P_{max}$ , maximum force consumption (kN)	48.1–176.4
$E_{max}$ , maximum energy consumption ( $kWh/m^3$ )	0.16–1.77
$K_{Lmax}$ , maximum linear cutting resistance (N/cm)	403.7–1276.7
$K_{Fmax}$ , maximum areal cutting resistance ( $N/cm^2$ )	43–285
Input Factors	Range of Values
$\gamma$ , coal unit weight ( $kN/m^3$ )	11.32–12.73
$\sigma_p$ , coal compressive strength (MPa)	4.11–6.26
$c$ , coal cohesion (Mpa)	0.83–1.67
$\varphi$ , coal angle of internal friction ( $^\circ$ )	38.27–48.39
$\varphi_L$ , excavator movement angle in the left direction ( $^\circ$ )	–76–90
$\varphi_D$ , excavator movement angle in the right direction ( $^\circ$ )	–76–90
$h$ , slice height (m)	2.8–5.5
$s$ , slice thickness (m)	0.15–3.0
$V_0$ , velocity of the rotary movement of the excavator (m/min)	6–22

There are 9 input factors for the developed DNN model. It contains three hidden layers, while the output of the model is in the form of a vector of 7 values (Figure 3). The three-layer DNN architecture is designed to capture a hierarchical representation of features within datasets. The first, second, and third hidden layers contain 256, 128, and 64 nodes, with sigmoid activation. After the first layer, a drop probability of 0.25 is applied, and after the second layer, a drop probability of 0.1 is used. The Adam optimizer is used during training, and the loss function is the mean square error (MSE) function. There were 300 epochs of training, with the following parameters:

- Parameter ReduceLROnPlateau, which reduces the learning rate if no accuracy on the validation dataset is improved for 35 epochs.
- Parameter EarlyStopping, which interrupts training if no accuracy is improved on the validation dataset for 45 epochs.

**Figure 3.** Deep neural network (DNN) model used for training.

The model was developed with a desktop PC with an Intel Core i9-9900K 3.60 Ghz CPU, 32 GB RAM, and an Nvidia GeForce RTX 2070 GPU.

### 3. Dependence of Each Output Factor on Controlling Parameters

#### 3.1. Performance of Bucket-Wheel Excavator

##### 3.1.1. Excavator Capacity $Q_{ef}$

The performed statistical analysis indicates that several two-factor interactions have statistically significant effects on  $Q_{ef}$  (Figure 4):

- Coal uniaxial compressive strength  $\sigma_p$ : It appears that  $\sigma_p$  has a variable effect on  $Q_{ef}$ , depending on the type of the parameter in the interaction. When  $\sigma_p$  is in interaction with the slice height ( $h$ ) and the excavator movement angle in the left direction ( $\varphi_L$ ),  $\sigma_p$  has a negative (decreasing) effect on  $Q_{ef}$ , meaning that excavator capacity decreases with the increase in  $\sigma_p$  (Figure 4a), which is expected. Such effect is obtained for the upper range of values of  $\sigma_p$  (6.00–6.30 MPa). However, when  $\sigma_p$  is in interaction with the coal friction angle  $\varphi$ , it appears that it has a positive effect on  $Q_{ef}$  (Figure 4c). This interesting finding could indicate that for high values of coal friction angles (above  $45.5^\circ$ ), an increase in  $\sigma_p$  leads to increase in  $Q_{ef}$ . One should note that this is achieved for the lower range of values of  $\sigma_p$  (4.00–4.60 MPa).
- Slice height  $h$ : It has a positive effect on  $Q_{ef}$  for all statistically significant two-factor interactions:  $\sigma_p$  (Figure 4a),  $c$  (Figure 4b), and  $s$  (Figure 4d), meaning that with the increase in slice height,  $Q_{ef}$  also increases.
- Excavator movement angle in the left direction ( $\varphi_L$ ): Similarly to slice height,  $\varphi_L$  also has a positive effect on  $Q_{ef}$  in all statistically significant interactions:  $\sigma_p$  (Figure 4a) and  $\varphi$  (Figure 4c).
- Velocity of the rotary movement of the excavator ( $V_0$ ):  $V_0$  has a negative effect on  $Q_{ef}$  in interaction with  $c$  (Figure 4b) and  $s$  (Figure 4d), meaning that  $Q_{ef}$  decreases as  $V_0$  increases.
- Coal cohesion ( $c$ ): It has a positive effect on  $Q_{ef}$  (Figure 4b), indicating that  $Q_{ef}$  increases as  $c$  increases. One should note that such an effect is captured for a relatively narrow range of values for cohesion (0.83–1.48 MPa).
- Coal friction angle ( $\varphi$ ): For medium values of  $\sigma_p$  (around 5 MPa),  $\varphi$  has a positive effect on  $Q_{ef}$  (Figure 4c). However, for low values of  $\sigma_p$  (4.00–4.30 MPa),  $\varphi$  has a negative effect on  $Q_{ef}$  (Figure 4c). However, one should note that the results of the ANOVA test indicate that the individual effect of the coal friction angle is statistically insignificant ( $p$ -value = 0.6374), so Figure 4c should be observed as relevant only for  $\varphi_L$  and  $\sigma_p$ : an increase in  $\varphi_L$  leads to an increase in  $Q_{ef}$  for all examined values of  $\varphi$ , while the increase in  $\sigma_p$  leads to an increase in  $Q_{ef}$  only for very high values of  $\varphi$  ( $>45.5^\circ$ ).
- Slice thickness ( $s$ ): Similar to slice height,  $s$  also has a positive effect on  $Q_{ef}$  in all statistically significant interactions:  $h$  and  $V_0$  (Figure 4d).

##### 3.1.2. Current Consumption $I_{max}$

The performed statistical analysis indicates that several two-factor interactions have statistically significant effects on  $I_{max}$  (Figure 5):

- Velocity of the rotary movement of the excavator ( $V_0$ ):  $V_0$  has a positive effect on  $I_{max}$ —an increase in  $V_0$  leads to an increase in  $I_{max}$  in interaction with the coal unit weight (Figure 5a) and friction angle (Figure 5c).
- Slice thickness ( $s$ ):  $s$  has a positive effect on  $I_{max}$  (Figure 5a).
- Coal unit weight ( $\gamma$ ):  $\gamma$  has a different effect on  $I_{max}$  depending on the parameter in co-action. When  $\gamma$  is interacting with  $c$  and  $V_0$ ,  $\gamma$  has a positive effect on  $I_{max}$  (Figure 5a). However, when  $\gamma$  is interacting with  $s$ , for lower values of  $s$ , the increase in  $\gamma$  has almost no effect on  $I_{max}$ . For higher values of  $s$ , the increase in  $\gamma$  leads to the decrease in  $I_{max}$ .

- Excavator movement angle: It has an opposite effect on  $I_{max}$ , depending on the excavation direction and coal compressive strength, which indicates specific geometry constraints and sedimentation conditions, which are favorable in the right direction of excavation for zones of coal with higher values of  $\sigma_p$  and in the left direction for zones of coal with lower values of  $\sigma_p$ :
  - Excavator movement angle in the left direction ( $\varphi_L$ ):  $\varphi_L$  has different effects for lower and medium-to-high values of  $\sigma_p$  (Figure 5b). For lower values of  $\sigma_p$ ,  $\varphi_L$  has a negative effect on  $I_{max}$ . However,  $\varphi_L$  has a positive effect on  $I_{max}$  for medium-to-high values of  $\sigma_p$ .
  - Excavator movement angle in the right direction ( $\varphi_D$ ):  $\varphi_D$  has different effects for lower and medium-to-high values of  $\sigma_p$  (Figure 5b). For lower values of  $\sigma_p$ ,  $\varphi_D$  has a positive effect on  $I_{max}$ . However,  $\varphi_D$  has a negative effect on  $I_{max}$  for medium-to-high values of  $\sigma_p$ .

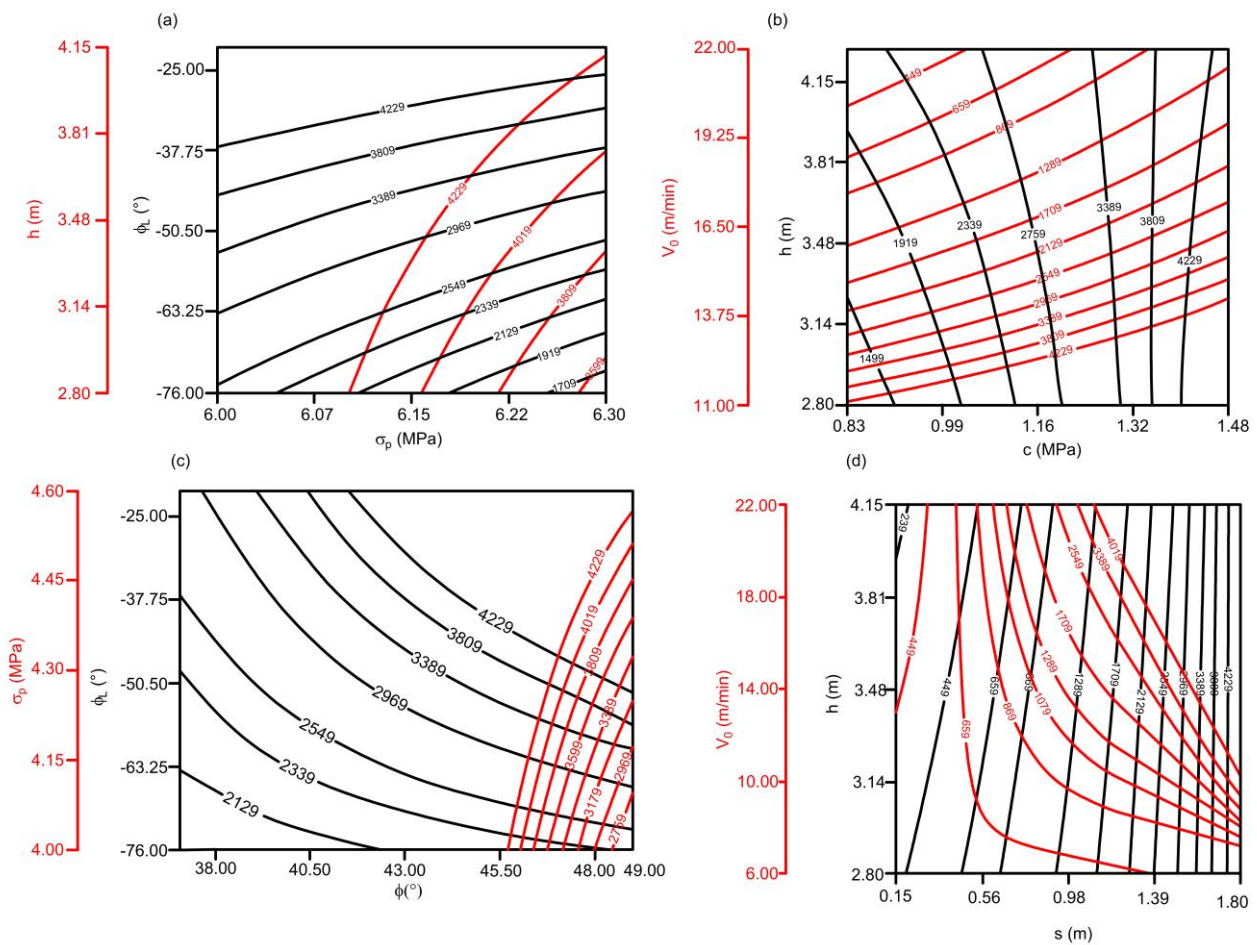


**Figure 4.** Statistically significant effect of different environmental properties and excavation parameters on excavator capacity  $Q_{ef}$ : (a)  $Q_{ef} = f(\sigma_p, \varphi_L, h)$ , (b)  $Q_{ef} = f(c, h, V_0)$ , (c)  $Q_{ef} = f(\sigma_p, \varphi_L, \varphi)$ , (d)  $Q_{ef} = f(V_0, h, s)$ . While the influential factors for each case are varied, other parameters are held constant for the fixed average values:  $\gamma = 12.02 \text{ kN/m}^3$ ,  $c = 1.25 \text{ MPa}$ ,  $\varphi_L = 7^\circ$ ,  $\varphi_D = 7^\circ$ ,  $h = 4.15 \text{ m}$ ,  $s = 1.58 \text{ m}$ ,  $V_0 = 14 \text{ m/min}$ ,  $\sigma_p = 5.19 \text{ MPa}$ ,  $\varphi = 43.33^\circ$ . Mutual two-factor interactions are obtained for high values of R (0.91) and low MSE (6.99).

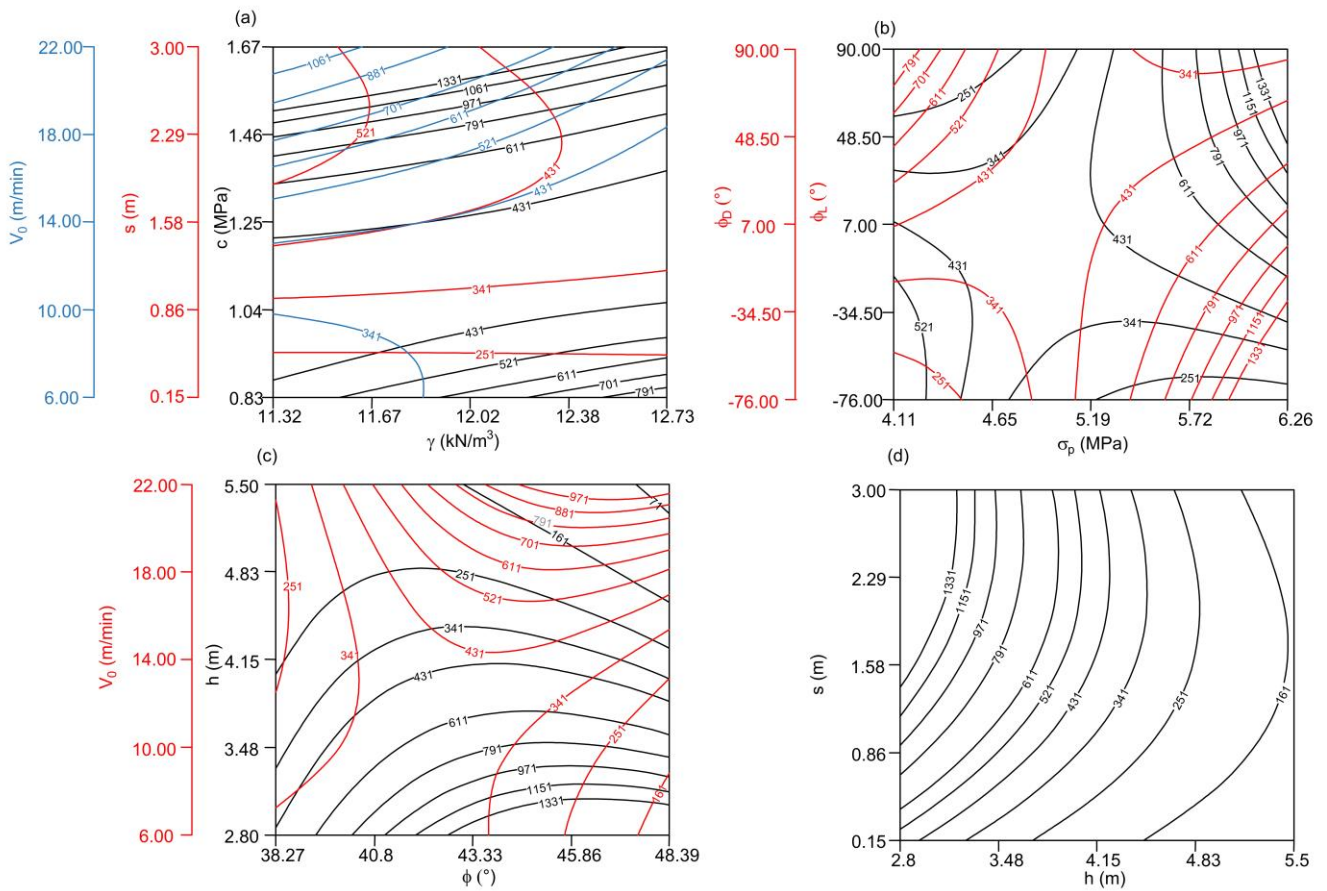


**Figure 5.** Statistically significant effect of different environmental properties and excavation parameters on maximum current consumption  $I_{max}$ : (a)  $I_{max} = f(\gamma, c, s, V_0)$ , (b)  $I_{max} = f(\sigma_p, \varphi_L, \varphi_D)$ , (c)  $I_{max} = f(\varphi, h, V_0)$ , (d)  $I_{max} = f(h, s)$ . While the influential factors for each case are varied, other parameters are held constant for the fixed average values:  $\gamma = 12.02 \text{ kN/m}^3$ ,  $c = 1.25 \text{ MPa}$ ,  $\varphi_L = 7^\circ$ ,  $\varphi_D = 7^\circ$ ,  $h = 4.15 \text{ m}$ ,  $s = 1.58 \text{ m}$ ,  $V_0 = 14 \text{ m/min}$ ,  $\sigma_p = 5.19 \text{ MPa}$ ,  $\varphi = 43.33^\circ$ . Mutual two-factor interactions are obtained for high values of R (0.98) and low MSE (5.63).

It should be noted that Figure 4b actually shows the same: excavation in the left direction is more favorable for zones of coal with higher  $\sigma_p$ , while excavation in the right direction is more favorable for zones of coal with lower  $\sigma_p$ .

- Coal compressive strength ( $\sigma_p$ ):  $\sigma_p$  has a different effect on  $I_{max}$  depending on the parameters in interaction and their values. When interacting with  $\varphi_D$ ,  $\sigma_p$  has a positive effect on  $I_{max}$  for medium-to-lower values of  $\varphi_D$ , while  $\sigma_p$  has a negative effect on  $I_{max}$  for higher values of  $\varphi_D$  (Figure 5b). When interacting with  $\varphi_L$ ,  $\sigma_p$  has a negative effect on  $I_{max}$  for medium-to-lower values of  $\varphi_L$ , while  $\sigma_p$  has a positive effect on  $I_{max}$  for higher values of  $\varphi_L$ . From the viewpoint of geomechanics, the relevant impact of  $\sigma_p$  is for the excavation angle in the left direction for  $\sigma_p$  higher than 5 MPa, where the increase in  $\sigma_p$  leads to the increase in  $I_{max}$ .
- Coal angle of internal friction ( $\varphi$ ): The effect of  $\varphi$  on  $I_{max}$  depends on the type of parameter in interaction and its values. For lower values of slice height  $h$ ,  $\varphi$  has a positive effect on  $I_{max}$ , while  $\varphi$  has a negative effect on  $I_{max}$  for medium-to-high values of  $h$  (Figure 5c). On the other hand, for medium-to-lower values of  $V_0$ ,  $\varphi$  has a negative effect on  $I_{max}$ , while  $\varphi$  has a positive effect on  $I_{max}$  for higher values of  $V_0$  (Figure 5c). However, according to the results of the ANOVA test, the individual effect of  $\varphi$  is statistically insignificant ( $p$ -value = 0.5541), so Figure 5 should be considered as relevant only for  $V_0$  and  $h$ , meaning that for all examined values of  $\varphi$ , an increase in  $V_0$  leads to an increase in  $I_{max}$ , while an increase in  $h$  leads to a decrease in  $I_{max}$ .

- Slice height ( $h$ ):  $h$  has a negative effect on  $I_{max}$  (Figure 5c,d). In particular, current consumption is lower for the higher values of slice height.

### 3.1.3. Power Consumption $N_{max}$

The performed statistical analysis indicates that several two-factor interactions have statistically significant effects on  $N_{max}$  (Figure 6):

- Velocity of the rotary movement of the excavator ( $V_0$ ):  $V_0$  has a positive effect on  $N_{max}$  (Figure 6c). Such a relationship is expected, indicating that the increase in  $V_0$  requires an increase in power consumption.
- Slice thickness ( $s$ ):  $s$  has a positive effect on  $N_{max}$ , regardless of the type of parameter in interaction (Figure 6a). In particular, an increase in slice thickness leads to an increase in  $N_{max}$ .
- Excavator movement angle in the left ( $\varphi_L$ ) and right ( $\varphi_D$ ) direction: It has a negative effect on  $N_{max}$ , regardless of the type of parameter in interaction (Figure 6b,c), which could be interpreted as a product of a specific geometry of the coal seam.
- Coal compressive strength ( $\sigma_p$ ):  $\sigma_p$  has a positive effect on  $N_{max}$  (Figure 6a), which indicates that the increase in  $\sigma_p$  leads to an increase in  $N_{max}$ .
- Coal cohesion ( $c$ ):  $c$  has a positive effect on  $N_{max}$ , regardless of the type of parameter in interaction (Figure 6b). In particular, an increase in coal cohesion leads to an increase in  $N_{max}$ .
- Coal angle of internal friction ( $\varphi$ ):  $\varphi$  has a negative effect on  $N_{max}$ , regardless of the type of parameter in interaction (Figure 6a,c). However, the ANOVA test indicated the statistically insignificant individual effect of  $\varphi$  ( $p$ -value = 0.0041). Therefore, Figure 6a,c should be considered as relevant only for  $s$  and  $V_0$ , meaning that  $N_{max}$  increases with the increase in  $V_0$  and  $s$  for all the examined values of coal friction angle.
- Slice height ( $h$ ):  $h$  has a negative effect on  $N_{max}$ , regardless of the type of parameter in interaction (Figure 6a,b). However, results of the ANOVA test indicate that  $h$  has statistically insignificant individual influence ( $p$ -value = 0.124), so the two-factor interactions should be considered as relevant only for  $c$ , meaning that an increase in cohesion leads to an increase in  $N_{max}$  for all the examined values of slice height.

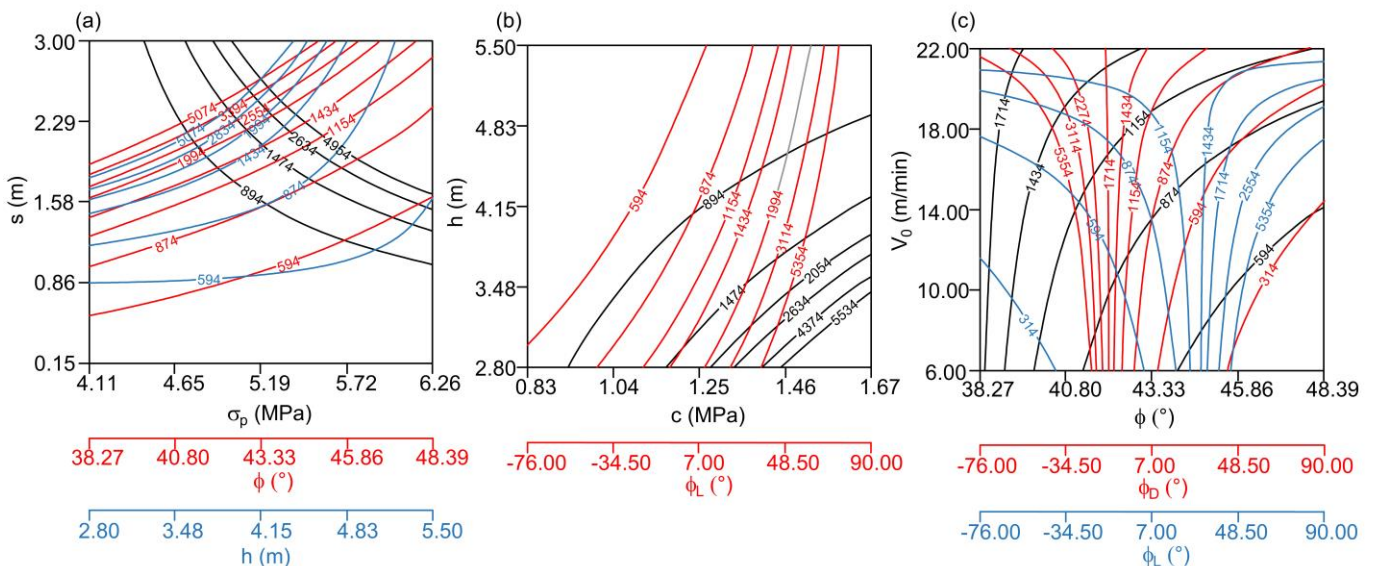


**Figure 6.** Statistically significant effect of different environmental properties and excavation parameters on maximum power consumption  $N_{max}$ : (a)  $N_{max} = f(\sigma_p, \varphi, s)$ , (b)  $N_{max} = f(c, h, \varphi_L)$ , (c)  $N_{max} = f(\varphi_D, \varphi_L, V_0)$ . While the influential factors for each case are varied, other parameters are held constant for the fixed average values:  $\gamma = 12.02 \text{ kN/m}^3$ ,  $c = 1.25 \text{ MPa}$ ,  $\varphi_L = 7^\circ$ ,  $\varphi_D = 7^\circ$ ,  $h = 4.15 \text{ m}$ ,  $s = 1.58 \text{ m}$ ,  $V_0 = 14 \text{ m/min}$ ,  $\sigma_p = 5.19 \text{ MPa}$ ,  $\varphi = 43.33^\circ$ . Mutual two-factor interactions are obtained for high values of R (0.77) and low MSE (0.00184).

### 3.1.4. Force Consumption $P_{max}$

The performed statistical analysis indicates that several two-factor interactions have statistically significant effects on  $P_{max}$  (Figure 7):

- Velocity of the rotary movement of the excavator ( $V_0$ ): The effect of  $V_0$  on  $P_{max}$  depends on the type of parameter in interaction and its values. For lower values of  $\sigma_p$ ,  $\varphi_D$ , and  $\varphi$ , an increase in  $V_0$  leads to a decrease in  $P_{max}$  (Figure 7a,c,d). However, for medium-to-high values of  $\sigma_p$ ,  $\varphi_D$ , and  $\varphi$ ,  $V_0$  has a positive effect on  $P_{max}$ .
- Slice thickness ( $s$ ):  $s$  has a positive effect on  $P_{max}$ , regardless of the parameter in interaction (Figure 7b,c). Such influence is expected because the increase in slice thickness should lead to an increase in  $P_{max}$ .
- Excavator movement angle: It has an opposite effect on  $P_{max}$ , depending on the excavation direction, which identifies specific geometry constraints and sedimentation conditions, which are favorable in the right direction of excavation:
  - Excavator movement angle in the left direction ( $\varphi_L$ ):  $\varphi_L$  has a positive effect on  $P_{max}$ , regardless of the parameter in interaction (Figure 7a,e).
  - Excavator movement angle in the right direction ( $\varphi_D$ ):  $\varphi_D$  has a negative effect on  $P_{max}$ , regardless of the parameter in interaction (Figure 7a,c).
- Coal compressive strength ( $\sigma_p$ ): An increase in  $\sigma_p$  from lower-to-medium values leads to a decrease in  $P_{max}$  in all interactions (Figure 7a,b). However, a further increase in  $\sigma_p$  from medium-to-high values leads to an increase in  $P_{max}$ . Therefore, one could conclude that relevant values of  $\sigma_p$  are higher than approximately 5 MPa.
- Coal angle of internal friction ( $\varphi$ ): An increase in  $\varphi$  from lower-to-medium values leads to an increase in  $P_{max}$  in interaction with  $h$  (Figure 7d). However, an increase in  $\varphi$  for lower-to-medium values of  $V_0$  leads to a decrease in  $P_{max}$  (Figure 7d). A further increase in  $\varphi$  for higher values of  $V_0$  leads to an increase in  $P_{max}$  (Figure 7d). One should note that according to the ANOVA test, the individual effect of the coal friction angle on  $P_{max}$  is statistically insignificant ( $p$ -value = 0.2113). However, the influence of two-factor interaction  $\varphi \times V_0$  is statistically significant ( $p$ -value = 0.005), while the impact of  $\varphi \times h$  should be taken with caution ( $p$ -value = 0.0587). Concerning this, one should consider the effect of the coal friction angle on  $P_{max}$  as relevant only for the lower values of  $\varphi$  (38–41°).
- Slice height ( $h$ ): for lower values of  $\sigma_p$ , an increase in  $h$  leads to an increase in  $P_{max}$ . For higher values of  $\sigma_p$ , an increase in  $h$  has almost no effect on  $P_{max}$  (Figure 7b). For lower-to-medium values of  $\varphi$ ,  $h$  has a positive effect on  $P_{max}$ , while  $h$  has a negative effect on  $P_{max}$  for higher values of  $\varphi$  (Figure 7d). For lower-to-medium values of  $\varphi_L$ , an increase in  $h$  leads to a decrease in  $P_{max}$ , while  $h$  has a positive effect on  $P_{max}$  for higher values of  $\varphi_L$  (Figure 7e).

### 3.1.5. Energy Consumption $E_{max}$

The performed statistical analysis indicates that several two-factor interactions have statistically significant effects on  $E_{max}$  (Figure 8):

- Velocity of the rotary movement of the excavator ( $V_0$ ):  $V_0$  has a negative effect on  $E_{max}$ , for all parameters in interaction, except for slice height, where a positive effect of  $V_0$  on  $E_{max}$  is recorded, for the medium-to-high values of  $V_0$  and medium-to-high values of slice height (Figure 8b).
- Slice thickness ( $s$ ):  $s$  has a negative effect on  $E_{max}$ , regardless of the parameters in interaction (Figure 8a,b). This means that the increase in slice thickness leads to a decrease in  $E_{max}$ . One should note that such an effect is obtained only for the range of  $s = 0.15$ – $0.64$  m, while for the higher values of  $s$  (0.64–1.20 m), slice thickness does not affect  $E_{max}$ .
- Coal unit weight ( $\gamma$ ): It has almost no effect on  $E_{max}$  (Figure 8a).
- Excavator movement angle in the right direction ( $\varphi_D$ ):  $\varphi_D$  has a negative effect on  $E_{max}$ , regardless of the parameters in interaction. This means that an increase in the excavator

- movement angle in the right direction leads to a decrease in  $E_{max}$ , which could be due to the specific geometry of the coal seam and/or particular sedimentation conditions.
- Slice height ( $h$ ):  $h$  has a positive effect on  $E_{max}$ , regardless of the parameters in interaction (Figure 8a,b). In particular, an increase in slice height leads to an increase in  $E_{max}$ , which is physically possible and expected.

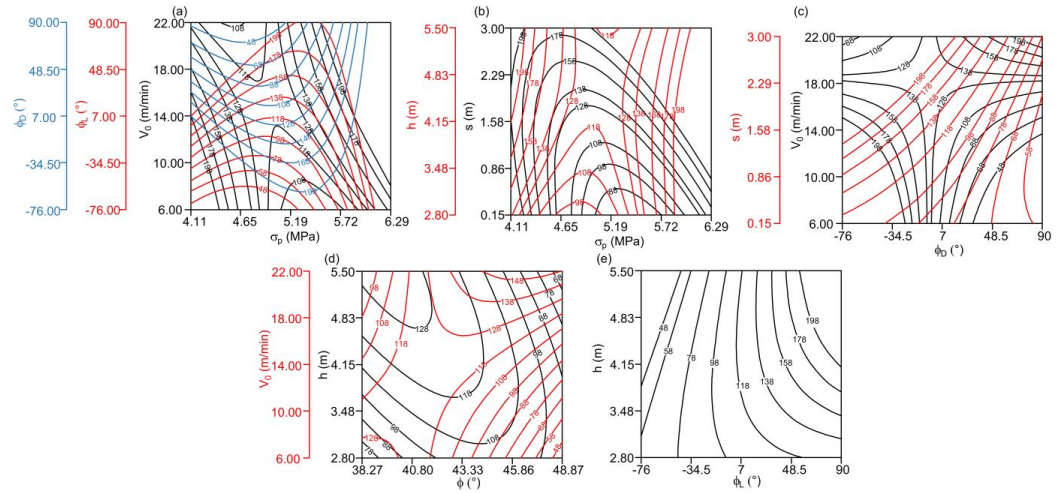


**Figure 7.** Statistically significant effect of different environmental properties and excavation parameters on maximum force consumption  $P_{max}$ : (a)  $P_{max} = f(\sigma_p, \varphi_D, \varphi_L, V_0)$ , (b)  $P_{max} = f(\sigma_p, h, s)$ , (c)  $P_{max} = f(\varphi_D, V_0, s)$ , (d)  $P_{max} = f(\varphi, V_0, h)$ , (e)  $P_{max} = f(\varphi_L, h)$ . While the influential factors for each case are varied, other parameters are held constant for the fixed average values:  $\gamma = 12.02 \text{ kN/m}^3$ ,  $c = 1.25 \text{ MPa}$ ,  $\varphi_L = 7^\circ$ ,  $\varphi_D = 7^\circ$ ,  $h = 4.15 \text{ m}$ ,  $s = 1.58 \text{ m}$ ,  $V_0 = 14 \text{ m/min}$ ,  $\sigma_p = 5.19 \text{ MPa}$ ,  $\varphi = 43.33^\circ$ . Mutual two-factor interactions are obtained for high values of R (0.86) and low MSE (10.43).

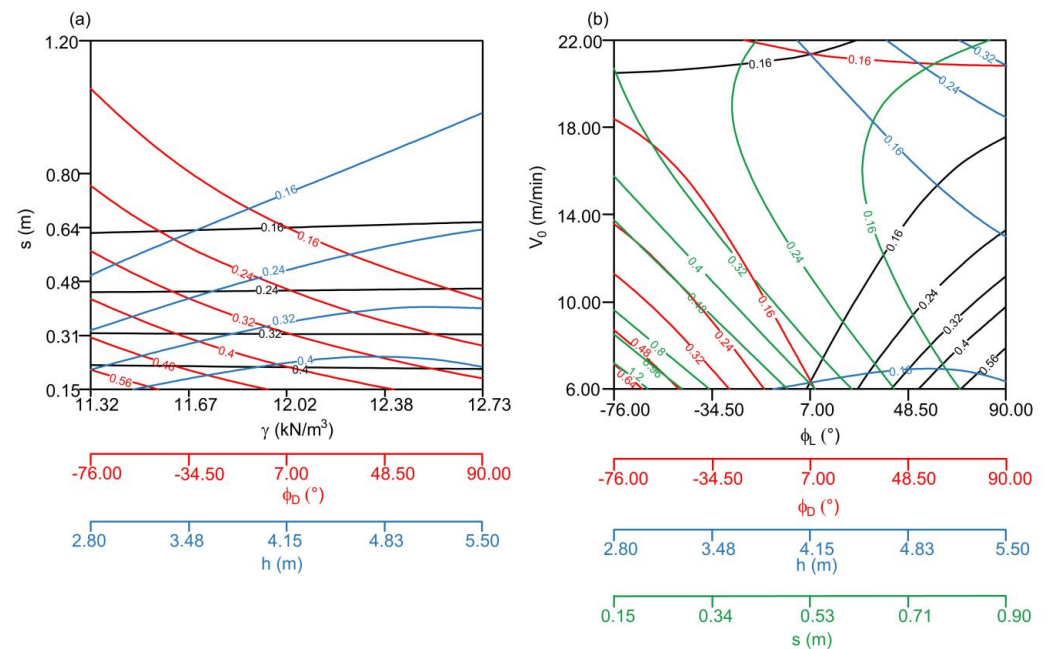


**Figure 8.** Statistically significant effect of different environmental properties and excavation parameters on maximum energy consumption  $E_{max}$ : (a)  $E_{max} = f(\varphi_D, h, s)$ , (b)  $E_{max} = f(\varphi_D, s, h, V_0)$ . While the influential factors for each case are varied, other parameters are held constant for the fixed average values:  $\gamma = 12.02 \text{ kN/m}^3$ ,  $c = 1.25 \text{ MPa}$ ,  $\varphi_L = 7^\circ$ ,  $\varphi_D = 7^\circ$ ,  $h = 4.15 \text{ m}$ ,  $s = 1.58 \text{ m}$ ,  $V_0 = 14 \text{ m/min}$ ,  $\sigma_p = 5.19 \text{ MPa}$ ,  $\varphi = 43.33^\circ$ . Mutual two-factor interactions are obtained for high values of R (0.95) and low MSE (0.82).

### 3.2. Cutting Resistance

#### 3.2.1. Linear Cutting Resistance $K_{Lmax}$

The performed statistical analysis indicates that several two-factor interactions have statistically significant effects on  $K_{Lmax}$  (Figure 9):

- Velocity of the rotary movement of the excavator ( $V_0$ ): For low  $\varphi_D$  and  $\sigma_p$ ,  $V_0$  has a negative effect on  $K_{Lmax}$  (Figure 9d,f). For medium-to-high values of  $\varphi_D$ , an increase in  $V_0$  leads to an increase in  $K_{Lmax}$ . On the other hand, for low-to-medium values of cohesion  $c$  and  $\varphi_L$ , an increase in  $V_0$  leads to an increase in  $K_{Lmax}$  (Figure 9e), while for higher values of  $c$ ,  $V_0$  has a negative effect on  $K_{Lmax}$ . There is a positive effect of  $V_0$  on  $K_{Lmax}$  for all values of the coal friction angle  $\varphi$ , except for very low values of  $\varphi$ , where an increase in  $V_0$  from low-to-medium values leads to a decrease in  $K_{Lmax}$ .
- Slice thickness ( $s$ ):  $s$  has a negative effect on  $K_{Lmax}$ , regardless of the parameters in interaction (Figure 9a,c). This means that an increase in slice thickness leads to a decrease in linear cutting resistance. However, if one takes a closer look at Figure 8a,c, it is clear that such an effect is captured only for low values of slice thickness. In particular, such effect is captured only for  $s = 0.15\text{--}1.5$  m and  $\sigma_p = 4.11\text{--}4.43$  MPa (Figure 9a); for higher values of  $s$ , slice thickness does not affect  $K_{Lmax}$ . Additionally, for higher values of  $h$  (Figure 9c), there is a negative effect on  $K_{Lmax}$ . However, one could say that in both figures,  $s$  predominantly does not affect  $K_{Lmax}$ .
- Coal unit weight ( $\gamma$ ): Unit weight has a positive effect on  $K_{Lmax}$  for lower values of  $c$  (Figure 9c). For higher values of  $c$ , unit weight does not affect  $K_{Lmax}$ . Indeed, an increase in unit weight should lead to an increase in linear cutting resistance.
- Excavator movement angle: It has an opposite effect on  $K_{Lmax}$ , depending on the excavation direction, which indicates specific geometry constraints and sedimentation conditions, which are favorable in the right direction of excavation:
  - Excavator movement angle in the left direction ( $\varphi_L$ ):  $\varphi_L$  has a positive effect on  $K_{Lmax}$ , regardless of the parameters in interaction (Figure 9a,b);
  - Excavator movement angle in the right direction ( $\varphi_D$ ):  $\varphi_D$  has a negative effect on  $K_{Lmax}$ , regardless of the parameters in interaction (Figure 9a,d).
- Coal compressive strength ( $\sigma_p$ ):  $\sigma_p$  has a negative effect on  $K_{Lmax}$  for all parameters in interaction (Figure 9a,f), except for a very high value of  $V_0$  (Figure 9f) when  $\sigma_p$  has a positive effect on  $K_{Lmax}$ . The effect of compressive strength is apparently physically possible only for the higher values of  $V_0$  because the increase in compressive strength should lead to the increase in  $K_{Lmax}$ .
- Coal cohesion ( $c$ ):  $c$  has a positive effect on  $K_{Lmax}$ , regardless of the parameters in interaction (Figure 9b,e). Such an effect is expected—an increase in cohesion should lead to an increase in  $K_{Lmax}$ .
- Slice height ( $h$ ):  $h$  has a positive effect on  $K_{Lmax}$ , regardless of the parameters in interaction (Figure 9b–d), except for the high values of  $\varphi_D$  when  $h$  does not affect  $K_{Lmax}$ . In particular, the increase in the slice height requires higher excavation power, which, further, reduces the cutting resistance.

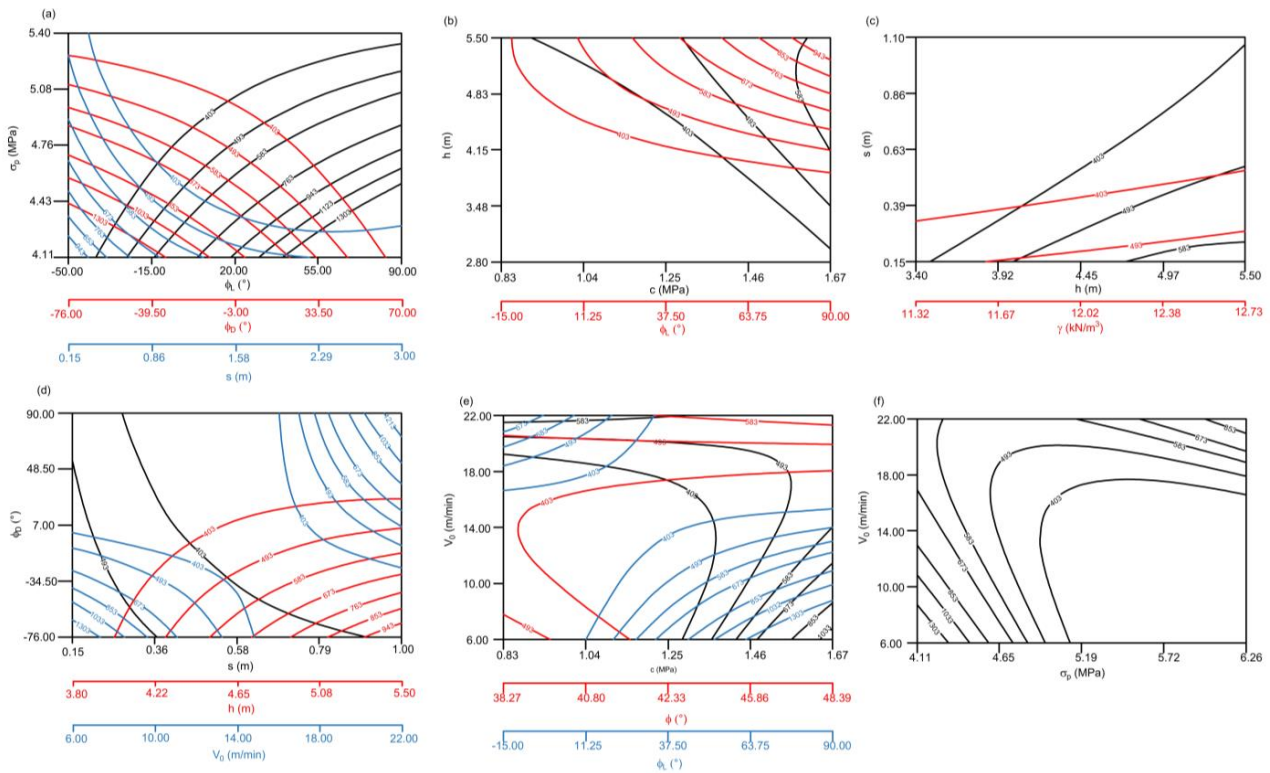


**Figure 9.** Statistically significant effect of different environmental properties and excavation parameters on maximum linear cutting resistance  $K_{Lmax}$ : (a)  $K_{Lmax} = f(\sigma_p, \varphi_D, s)$ , (b)  $K_{Lmax} = f(\varphi_L, c, h)$ , (c)  $K_{Lmax} = f(\gamma, h, s)$ , (d)  $K_{Lmax} = f(\varphi_D, h, s, V_0)$ , (e)  $K_{Lmax} = f(\varphi, \varphi_L, V_0)$ , (f)  $K_{Lmax} = f(\sigma_p, V_0)$ . While the influential factors for each case are varied, other parameters are held constant for the fixed average values:  $\gamma = 12.02 \text{ kN/m}^3$ ,  $c = 1.25 \text{ MPa}$ ,  $\varphi_L = 7^\circ$ ,  $\varphi_D = 7^\circ$ ,  $h = 4.15 \text{ m}$ ,  $s = 1.58 \text{ m}$ ,  $V_0 = 14 \text{ m/min}$ ,  $\sigma_p = 5.19 \text{ MPa}$ ,  $\varphi = 43.33^\circ$ . Mutual two-factor interactions are obtained for high values of R (0.73) and low MSE (6.57).

### 3.2.2. Areal Cutting Resistance $K_{Fmax}$

The performed statistical analysis indicates that several two-factor interactions have statistically significant effects on  $K_{Fmax}$  (Figure 10):

- Velocity of the rotary movement of the excavator ( $V_0$ ):  $V_0$  has a negative effect on  $K_{Fmax}$ , regardless of the parameters in interaction (Figure 10c,d). Such an effect is expected, because the increased wheel velocity indicates higher power and, thus, lower cutting resistance.
- Slice thickness ( $s$ ):  $s$  has a negative effect on  $K_{Fmax}$ , regardless of the parameters in interaction (Figure 10b,d). This means that the increase in slice thickness leads to a decrease in areal cutting resistance. However, one should note that such an effect is observed only for low values of slice thickness (below 1 m), so it could be said that predominantly  $s$  has no effect on  $K_{Fmax}$ .
- Coal unit weight ( $\gamma$ ):  $\gamma$  has a positive effect on  $K_{Fmax}$  (Figure 10d). From a geometrical viewpoint, such an effect is expected: the increase in unit weight leads to the increased cutting resistance.
- Excavator movement angle in the left direction ( $\varphi_L$ ):  $\varphi_L$  has a positive effect on  $K_{Fmax}$ , regardless of the parameters in interaction (Figure 10a,c). In a particular case, it means that the increase in the movement angle in the left direction leads to the increase in cutting resistance, which could be ascribed to the specific geometry of the coal seam and inherent sedimentation conditions.
- Excavator movement angle in the right direction ( $\varphi_D$ ):  $\varphi_D$  has a different effect on  $K_{Fmax}$ , depending on the type of parameter in interaction. In interaction with  $\sigma_p$  and  $h$ ,  $\varphi_D$  has a negative effect on  $K_{Fmax}$ . In particular, for higher values of  $h$  (4.60–5.50 m), an

increase in  $\varphi_D$  leads to a decrease in  $K_{Fmax}$ . This effect is the same for lower values of  $\sigma_p$  (4.11–4.81 MPa). In interaction with  $s$ ,  $\varphi_D$  has a positive effect on  $K_{Fmax}$ , which is identical to the influence in the case of  $\varphi_L$ .

- Coal cohesion ( $c$ ):  $c$  has a positive effect on  $K_{Fmax}$  (Figure 10b). Such effect is expected because the increase in cohesion of the coal indeed leads to the increase in the areal cutting resistance.
- Coal angle of internal friction ( $\varphi$ ):  $\varphi$  has a negative effect on  $K_{Fmax}$  (Figure 10c). One would expect that because cohesion has a positive effect on  $K_{Fmax}$ , such influence is expected also for the friction angle. However, resistance to failure during the cutting is obviously determined by cohesion, while, once the failure is achieved during the cutting process, shear strength does not affect  $K_{Fmax}$ . Figure 10c should be observed as relevant only for wheel velocity  $V_0$ , meaning that the increase in  $V_0$  for any value of  $\varphi$  leads to a decrease in  $K_{Fmax}$ . This is further proven by the ANOVA test, which indicates a much smaller  $p$ -value for  $V_0$  (0.0096) compared to the  $p$ -value for  $\varphi$  (0.0631). The  $p$ -value of  $V_0 \times \varphi$  is also relatively high (0.0614).
- Slice height ( $h$ ):  $h$  has a positive effect on  $K_{Fmax}$ , regardless of the parameters in interaction (Figure 10a,c). In particular, the increase in the slice height requires higher excavation power, which, further, reduces the cutting resistance.

### 3.3. Analysis of the Most Significant Factors

Based on the performed multiple linear regression analysis, whose results are shown in Sections 3.1 and 3.2, one could single out the most important two-factor interactions affecting the chosen parameters of coal cutting resistance and excavator performance. Significant two-factor interactions are singled out according to the lowest  $p$ -value (Table 2).

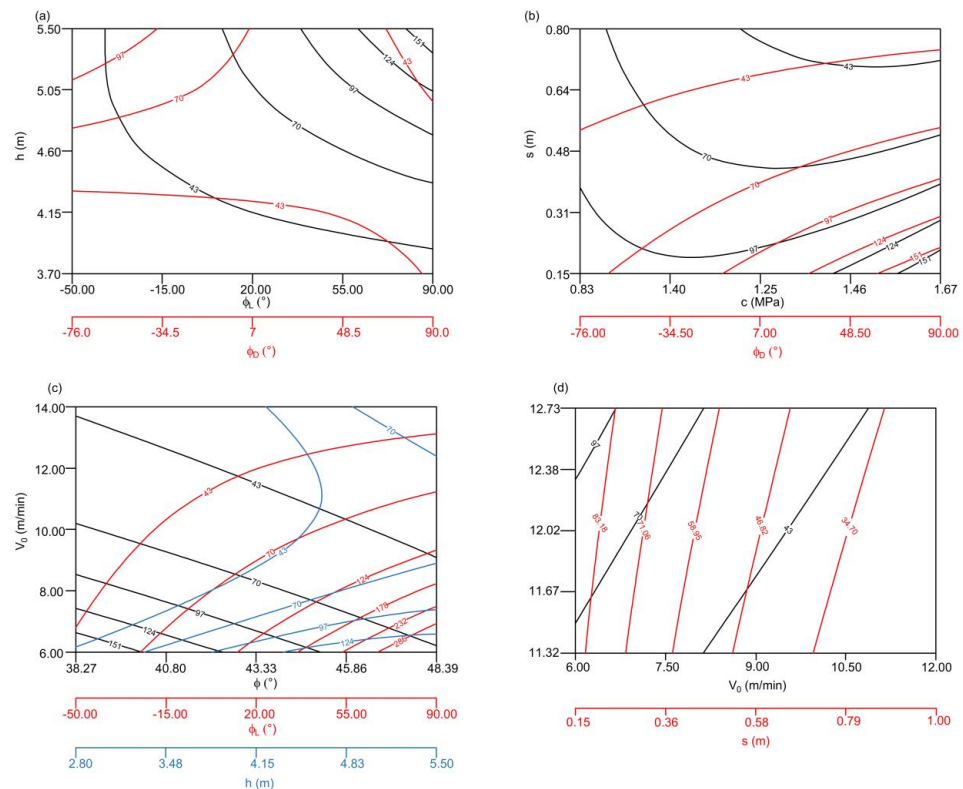


**Figure 10.** Statistically significant effect of different environmental properties and excavation parameters on maximum areal cutting resistance  $K_{Fmax}$ : (a)  $K_{Fmax} = f(\varphi_L, \varphi_D, h)$ , (b)  $K_{Fmax} = f(\varphi_D, c, s)$ , (c)  $K_{Fmax} = f(\varphi_L, h, V_0)$ , (d)  $K_{Fmax} = f(\gamma, V_0, s)$ . While the influential factors for each case are varied, other parameters are held constant for the fixed average values:  $\gamma = 12.02$  kN/m<sup>3</sup>,  $c = 1.25$  MPa,  $\varphi_L = 7^\circ$ ,  $\varphi_D = 7^\circ$ ,  $h = 4.15$  m,  $s = 1.58$  m,  $V_0 = 14$  m/min,  $\sigma_p = 5.19$  MPa,  $\varphi = 43.33^\circ$ . Mutual two-factor interactions are obtained for high values of R (0.75) and low MSE (4.63).

**Table 2.** The most statistically significant two-factor interactions.

Significant Input Factors ( $p < 0.0001$ )	Output Factors
$\varphi_L \times V_0$	$N_{max}, P_{max}, E_{max}, K_{Lmax}$
$\varphi_D \times V_0$	$N_{max}, E_{max}, K_{Lmax}, P_{max}$
$\sigma_p \times \varphi_L$	$Q_{ef}, I_{max}, K_{Lmax}$
$\varphi_L \times \varphi_D$	$Q_{ef}, E_{max}$
$c \times h$	$I_{max}, K_{Lmax}$
$\varphi_D \times h$	$K_{Lmax}, K_{Fmax}$
$\sigma_p \times \varphi_D$	$I_{max}$
$\varphi_D \times s, h \times s, s \times V_0$	$E_{max}$
$c \times V_0$	$K_{Lmax}$
$\sigma_p \times V_0$	$K_{Fmax}$

As one can see from Table 2, excavator movement angle in both directions, wheel velocity, and coal compressive strength are the most significant factors affecting all the examined output factors. Such an important influence of  $\varphi_L$  and  $\varphi_D$  could be ascribed to the specific geometry of the coal seam, its spatial distribution, and particular internal structure. The important effect of  $V_0$  and  $\sigma_p$  on the excavator performance and coal cutting resistance is expected and verified in the present research.

Coal cohesion and slice height also have a significant influence, but only for some of the output factors, while slice thickness has the most important impact on maximum energy consumption.

On the other hand, one can see that coal unit weight and angle of internal friction do not occur as the most significant influential factors. In general, the unit weight of coal changes in a small range, which commonly does not affect the important geomechanical properties of coal and the excavator performance. As for the friction angle, the results of the present research indicate the following: once the part of coal shear strength attributed to cohesion is overcome by the excavator, friction angle does have such a significant influence in the subsequent excavation process.

#### 4. Development of a Model Based on Deep Neural Networks

In this research, deep neural networks (DNNs) have been devised to extrapolate a sequence of excavation parameters, depending on the main environmental and excavation properties. The model choice is selected based on the guidelines provided by Bergen et al. [19], Reichstein et al. [20], and Mignan and Broccardo [21], primarily attributed to the capability of DNN models in capturing complex, nonlinear relationships and identifying patterns within expansive datasets, notably within the realm of engineering disciplines such as earth science engineering.

Utilizing a three-layer DNN architecture is motivated by the aim of leveraging the DNN's capability to capture hierarchical features inherent in the datasets. Specifically, the first layer is tuned to detect rudimentary or low-level attributes, the subsequent layer identifies intermediate or medium-level features, and the final layer focuses on advanced, high-level, or abstract characteristics [22]. By reducing the number of nodes in deeper layers from 256 and 128 to 64, DNNs are inclined to prioritize and retain only the most critical information, leading to a streamlined and concise representation of the data [23,24]. A higher dropout rate of 0.25 is assigned to the first layer, which has the most nodes, while for the second and third layers, a dropout rate of 0.1 is employed. This choice is motivated by the fact that the initial layer, capturing rudimentary or low-level attributes, possesses a broader and more diversified set of features, while the next two layers systematically transform the extensive input data into more detailed estimates [25].

Regarding the optimization of DNNs, the Adam optimizer is particularly favored due to its capability to effectively manage the complexities of large parameter spaces and layered architectures, thus offering superior performance in comparison to other optimization methods [25]. In contrast to alternatives like Gradient Descent, Stochastic Gradient Descent, and Adagrad, Adam excels by combining the benefits of adaptive learning rates, often resulting in more rapid convergence and superior performance in DNNs.

The adequate architecture of the neural network is determined based on the following. Three different optimization algorithms are examined, among which Adam's optimization algorithm is chosen, as the one with the lowest MSE (Table 3).

**Table 3.** MSE of the DNN model with different optimization algorithms.

Optimization Algorithm	MSE (Training)	MSE (Test)
Adam [26]	0.0121	0.0191
AdaDelta [25]	0.0434	0.0432
SDG [27]	0.0425	0.0431

For the Adam optimization algorithm, four different architectures are tested, with different numbers of nodes per hidden layer (Table 4). It is clear from Table 4 that the Adam optimization algorithm with 256, 128, and 64 nodes per hidden layer has the lowest MSE.

**Table 4.** MSE of the DNN model with a different number of nodes per hidden layer.

Model Configuration	MSE (Training)	MSE (Test)
512, 256, 128, Adam	0.0142	0.0206
256, 128, 64, Adam	0.0121	0.0192
128, 64, 32, Adam	0.0113	0.0198
64, 32, 16, Adam	0.0210	0.0199

The chosen DNN model with the determined architecture undergoes training over 300 epochs to determine the optimal parameters for prediction. The overall efficiency of the model parameters, using mean square error (MSE), is evaluated across all modeling parameters (Figure 3) and depicted in Figure 11. It is evident that the MSE decreases sharply up to roughly 50 epochs, and upon increasing further epochs, it stabilizes to relatively consistent MSE values (Figure 11).

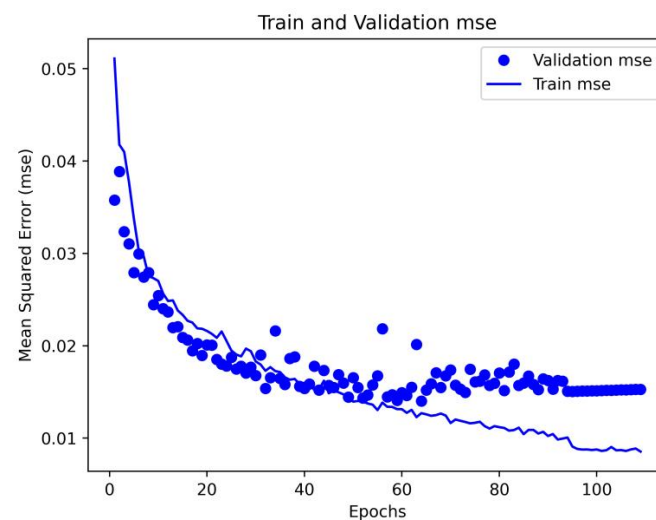


**Figure 11.** Training and validation of the DNN model using mean square error (MSE) as the optimization criterion over epochs.

Once the DNN model is selected, its efficiency is assessed for six variables:  $Q_{ef}$ ,  $N_{max}$ ,  $P_{k,max}$ ,  $E_{max}$ ,  $K_{L,max}$ , and  $K_{F,max}$  (Figure 12). During model training, the MSE ranges between 6.7% and 11.5%, indicating that the model is suitable for all the variables. The highest matching between the expected and predicted variables is observed for  $N_{max}$  (Figure 12b), whereas the model’s performance for  $K_{F,max}$  suggests the least but relatively good alignment with the expected variable (Figure 12f).

When tested with an unseen dataset, the DNN model validation indicates satisfactory results, with MSE values between 9.2% and 16.5% (Figure 13). The highest correspondence is seen for  $N_{max}$ , consistent with the training dataset (Figure 13b). On the other hand, while the alignment for  $E_{max}$  (Figure 13d) and  $K_{F,max}$  (Figure 13f) is on the lower side, it is still reasonable at 16.5% and 16.4%, respectively.

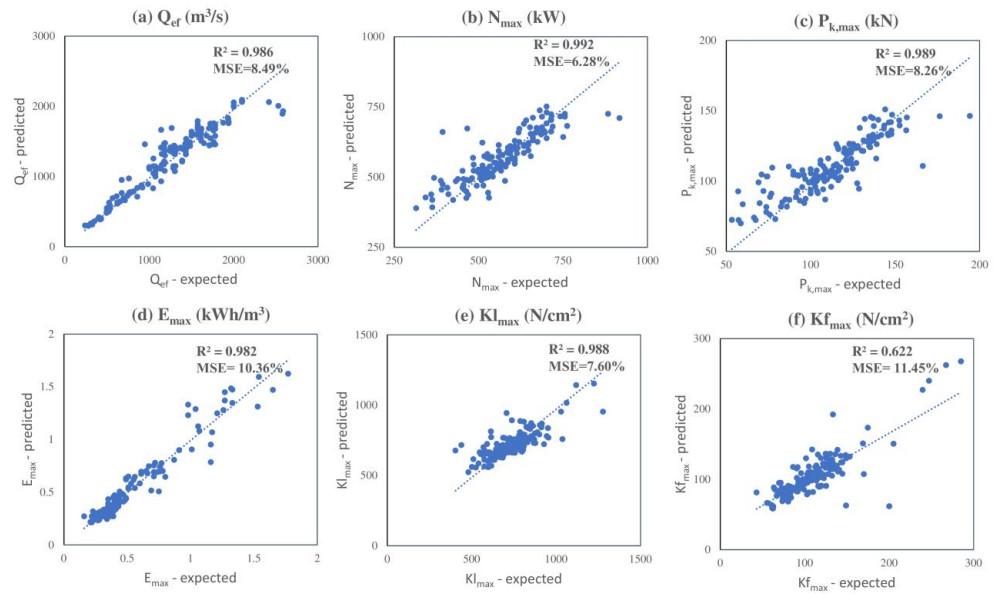


**Figure 12.** Results from the DNN model training for variables: (a)  $Q_{ef}$ , (b)  $N_{max}$ , (c)  $P_{k,max}$ , (d)  $E_{max}$ , (e)  $K_{L,max}$ , and (f)  $K_{F,max}$ .

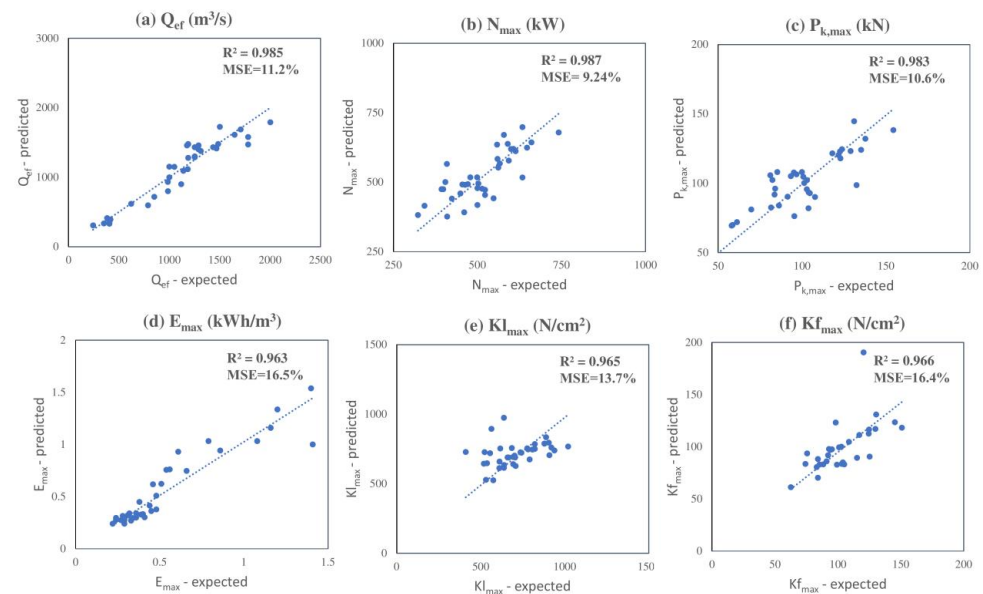


**Figure 13.** Results from DNN model verification: (a)  $Q_{ef}$ , (b)  $N_{max}$ , (c)  $P_{k,max}$ , (d)  $E_{max}$ , (e)  $K_{L,max}$ , and (f)  $K_{F,max}$ .

For  $E_{max}$ , the mean squared error (MSE) stands at 10.36%. For  $K_{Fmax}$ , it is slightly lower at 7.6%. The  $R^2$  values for these variables are 0.982 and 0.988, respectively. For  $K_{Fmax}$ , when the predicted and expected values range from 500 to 1000 N/cm<sup>2</sup>, the model performs well. Outside of this range, the model tends to have higher errors. In the case of  $E_{max}$ , for values exceeding 1 kWh/m<sup>3</sup>, there is a divergence between the predicted and expected values, which contributes to the MSE of 10.36%. Nevertheless, based on the  $R^2$  and MSE values, the modeling performance can be deemed robust and effective, especially within the anticipated ranges ( $K_{Fmax}$  between 500 and 1000 N/cm<sup>2</sup> and  $E_{max}$  up to 1 kWh/cm<sup>3</sup>)

The outcomes of the DNN model for the variable  $I_{max}$  are presented distinctly. This is due to the unique characteristic of the  $I_{max}$  values which can be either extremely low or high. For a more concise representation, Figure 14 displays promising results with an MSE between 4.8% and 12.5%.

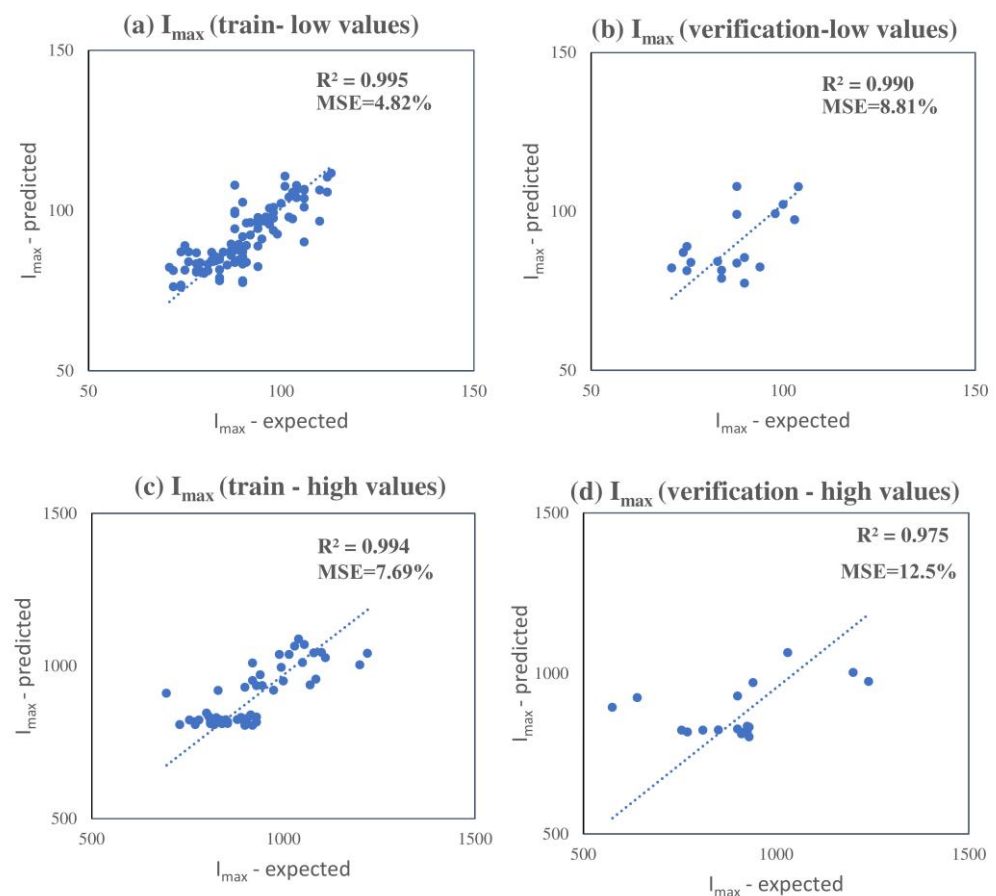


**Figure 14.** Results from the DNN model test and verification for  $I_{max}$ : (a) training of model of low values, (b) verification of model of low values; (c) training of model of high values; (d) verification of model of high values.

## 5. Conclusions

The results of the performed analysis indicate that some of the controlling factors do not have a statistically significant effect on some of the output factors, i.e.,:

- Coal unit weight  $\gamma$  has a statistically significant effect only for the current consumption  $I_{max}$ , areal cutting resistance  $K_{Fmax}$ , and for the linear cutting resistance  $K_{Lmax}$  for low values of coal cohesion. For all the rest of the output factors,  $\gamma$  does not have a statistically significant influence.
- Coal cohesion  $c$  has a statistically significant effect only for the excavator capacity  $Q_{ef}$ , power consumption  $N_{max}$ , and linear and areal cutting resistance of coal,  $K_{Lmax}$  and  $K_{Fmax}$ .

- Coal angle of internal friction  $\varphi$  does not have a statistically significant effect on energy consumption  $E_{max}$  and linear cutting resistance  $K_{Lmax}$ .
- Coal compressive strength  $\sigma_p$  does not have a statistically significant influence on energy consumption  $E_{max}$  and areal cutting resistance  $K_{Fmax}$ .
- Excavator movement angle in the right direction ( $\varphi_D$ ) does not have a statistically significant influence on excavator capacity  $Q_{ef}$ .

All parameters have a certain effect on output factors, independent of the quality of the two-factor interaction, or dependent on the values of the other interacting controlling factors:

- Velocity of the rotary movement of the excavator ( $V_0$ ):
  - $V_0$  has a negative effect (meaning that the output parameter decreases as  $V_0$  increases) on (1)  $Q_{ef}$  in interaction with  $c$  and  $s$ ; (2)  $P_{max}$ , for lower values of  $\sigma_p$ ,  $\varphi_D$ , and  $\varphi$ ; (3)  $E_{max}$ , for all parameters in interaction, except for moderate-to-high values of slice height; (4)  $K_{Lmax}$ , for low-to-medium values of cohesion  $c$  and  $\varphi_L$ , and for higher values of  $c$  and  $V_0$  and very low values of  $\varphi$ ; and (5)  $K_{Fmax}$ ;
  - $V_0$  has a positive effect (meaning that the output parameter increases as  $V_0$  increases) on (1)  $I_{max}$ ; (2)  $N_{max}$ ; (2)  $P_{max}$ , for medium-to-high values of  $\sigma_p$ ,  $\varphi_D$ , and  $\varphi$ ; (3)  $E_{max}$ , for medium-to-high values of slice height; and (4)  $K_{Lmax}$ , for low-to-medium values of cohesion  $c$  and  $\varphi_L$ .
- Slice thickness ( $s$ ):
  - $s$  has a negative effect (meaning that the output parameter decreases as  $s$  increases) on  $E_{max}$ ,  $K_{Lmax}$ , and  $K_{Fmax}$ ;
  - $s$  has a positive effect (meaning that the output parameter increases as  $s$  increases) on  $Q_{ef}$ ,  $I_{max}$ ,  $N_{max}$ , and  $P_{max}$ .
- Coal unit weight ( $\gamma$ ):
  - $\gamma$  has a negative effect (meaning that the output parameter decreases as  $\gamma$  increases) on  $I_{max}$ , for higher values of slice thickness  $s$ ;
  - $\gamma$  has a positive effect (meaning that output parameter increases as  $\gamma$  increases) on (1)  $I_{max}$ , except for the higher values of  $s$ ; (2)  $K_{Lmax}$ , for lower values of cohesion; and (3)  $K_{Fmax}$ .
- Excavator movement angle in the left direction ( $\varphi_L$ ):
  - $\varphi_L$  has a negative effect (meaning that the output parameter decreases as  $\varphi_L$  increases) on (1)  $I_{max}$ , for lower values of  $\sigma_p$ , and (2)  $N_{max}$ ;
  - $\varphi_L$  has a positive effect (meaning that the output parameter increases as  $\varphi_L$  increases) on  $Q_{ef}$ ,  $I_{max}$  (for moderate to high values of  $\sigma_p$ ),  $P_{max}$ ,  $K_{Lmax}$ , and  $K_{Fmax}$ .
- Excavator movement angle in the right direction ( $\varphi_D$ ):
  - $\varphi_D$  has a negative effect (meaning that the output parameter decreases as  $\varphi_D$  increases) on  $I_{max}$  (for medium-to-high values of  $\sigma_p$ ),  $N_{max}$ ,  $P_{max}$ ,  $E_{max}$ ,  $K_{Lmax}$ , and  $K_{Fmax}$  (in interaction with  $\sigma_p$  and  $h$ );
  - $\varphi_D$  has a positive effect (meaning that the output parameter increases as  $\varphi_D$  increases) on  $I_{max}$  (for lower values of  $\sigma_p$ ) and  $K_{Fmax}$  (in interaction with  $s$ ).
- Coal compressive strength ( $\sigma_p$ ):
  - $\sigma_p$  has a negative effect (meaning that the output parameter decreases as  $\sigma_p$  increases) on (1)  $Q_{ef}$ , in interaction with slice height ( $h$ ) and excavator movement angle in the left direction ( $\varphi_L$ ); (2)  $I_{max}$ , for higher values of  $\varphi_D$  and for medium-to-lower values of  $\varphi_L$ ; (3)  $P_{max}$ , for lower-to-medium values of  $\sigma_p$ ; and (4)  $K_{Lmax}$ , except for very high values of  $V_0$ ;
  - $\sigma_p$  has a positive effect (meaning that the output parameter increases as  $\sigma_p$  increases) on (1)  $Q_{ef}$ , in interaction with friction angle, for a lower range of values of  $\sigma_p$  (4.00–4.60 MPa); (2)  $I_{max}$ , for medium-to-lower values of  $\varphi_D$  and

for higher values of  $\varphi_L$ ; (3)  $N_{max}$ ; (4)  $P_{max}$ , for moderate-to-high values of  $\sigma_p$ ; and (5)  $K_{Lmax}$ , for very high values of  $V_0$ .

- Coal cohesion ( $c$ ):
  - $c$  has no negative effect on the output parameters;
  - $c$  has a positive effect (meaning that the output parameter increases as  $c$  increases) on  $Q_{ef}$ ,  $N_{max}$ ,  $K_{Lmax}$ , and  $K_{Fmax}$ .
- Coal angle of internal friction ( $\varphi$ ):
  - $\varphi$  has a negative effect (meaning that the output parameter decreases as  $\varphi$  increases) on (1)  $Q_{ef}$ , for low values of  $\sigma_p$  (4.00–4.30 MPa); (2)  $I_{max}$ , for medium-to-high values of  $h$  and for medium-to-lower values of  $V_0$ ; (3)  $N_{max}$ ; (4)  $P_{max}$ , for lower-to-medium values of  $V_0$ ; and (5)  $K_{Fmax}$ ;
  - $\varphi$  has a positive effect (meaning that the output parameter increases as  $\varphi$  increases) on (1)  $Q_{ef}$ , for medium values of  $\sigma_p$  (around 5 MPa); (2)  $I_{max}$ , for lower values of slice height  $h$  and higher values of  $V_0$ ; and (3)  $P_{max}$ , for lower-to-medium values of  $\varphi$  and for higher values of  $V_0$ .
- Slice height ( $h$ ):
  - $h$  has a negative effect (meaning that the output parameter decreases as  $h$  increases) on  $I_{max}$ ,  $N_{max}$ , and  $P_{max}$  (for higher values of  $\varphi$  and for lower-to-medium values of  $\varphi_L$ );
  - $h$  has a positive effect (meaning that the output parameter increases as  $h$  increases) on  $Q_{ef}$ ;  $P_{max}$  (for lower values of  $\sigma_p$  and for lower-to-medium values of  $\varphi$ , and for higher values of  $\varphi_L$ );  $E_{max}$ ;  $K_{Lmax}$ , except for the high values of  $\varphi_D$ ; and  $K_{Fmax}$ .

The DNN joint model for estimation of excavator performance and coal cutting resistance has three hidden layers (256, 128, and 64 nodes) with drop rates of 0.25 and 0.1, and it was trained using the Adam optimizer and MSE for 300 epochs. The DNN model's efficiency showed decreasing MSE up to ~50 epochs before stabilizing. When assessed for six examined variables, the model had an MSE between 6.7% and 11.5%, with the best match for  $N_{max}$ . On unseen data, results remained consistent, with MSEs between 9.2% and 16.5%. The variable  $I_{max}$ , due to its distinct low or high values, is separately visualized, yielding a 4.8% to 12.5% MSE range.

The model developed in the present study, including the determined complex relations between different parameters of the excavation process and coal properties, could be further used for both planning and optimization of the coal exploitation process. In particular, the planning process for long-term operation at open-pit coal mines could be significantly improved because the choice of the adequate type of bucket-wheel excavator could be made based on the estimated performances. As for the optimization process, it is possible to estimate the excavation performance of the bucket-wheel excavator solely based on laboratory-determined coal properties. Moreover, a required parameter of the excavation performance could be roughly estimated solely by addressing the single most significant parameter of the coal. The DNN model presented in this study, although it is developed for the specific location, could be updated with new parameter values and used for estimation of performance cutting resistance at any other open-pit surface mine with similar geological conditions as the one examined in the present paper.

**Author Contributions:** All authors contributed to the study's conception and design. Analysis of the effect of each influential factor was performed by S.K. and J.T. Development of the DNN model was performed by V.I., S.K. and M.S. wrote the first draft of the manuscript. All authors commented on previous versions of the manuscript. All authors have read and agreed to the published version of the manuscript.

**Funding:** This research received no external funding.

**Data Availability Statement:** Data used or generated within this study will be made available upon reasonable request.

**Conflicts of Interest:** The authors declare no conflict of interest.

## References

1. Gordon, L.R. *World Coal. Economics, Policies and Prospects*; Cambridge University Press: London, UK, 1987.
2. Available online: <https://ember-climate.org/data-catalogue/yearly-electricity-data/> (accessed on 15 August 2023).
3. Available online: <https://ember-climate.org/insights/research/european-electricity-review-2022/> (accessed on 15 August 2023).
4. Available online: <https://www.energyinst.org/statistical-review/> (accessed on 15 August 2023).
5. Ritchie, H. The Death of UK Coal in Five Charts. Available online: <https://ourworldindata.org/death-uk-coal> (accessed on 8 August 2023).
6. Liu, X.; Li, L.; Yang, Y. Development status of coal mining in China. *J. South. African Inst. Min. Metal.* **2023**, *123*, 19–28. [[CrossRef](#)]
7. Vujić, S. (Ed.) *Serbian Mining and Geology in the Second Half of the XX Century*; Academy of Engineering Science of Serbia, Matica Srpska and Mining Institute: Belgrade, Serbia, 2014. (In Serbian)
8. Andraş, A.; Radu, S.M.; Brînaş, I.; Popescu, F.D.; Budilicã, D.I.; Korozsi, E.B. Prediction of Material Failure Time for a Bucket Wheel Excavator Boom Using Computer Simulation. *Materials* **2021**, *14*, 7897. [[CrossRef](#)] [[PubMed](#)]
9. Jiang, Y.; Liao, G.; Zhu, S.; Hu, Y. Investigation on Cutting Resistance Characteristic of Bucket Wheel Excavator Using DEM and DOE Methods. *Simul. Model. Pract. Theory* **2021**, *111*, 102339.
10. Popescu, F.D.; Radu, S.M.; Kotwica, K.; Andraş, A.; Kertesz, I. Simulation of the Time Response of the ERc 1400-30/7 Bucket Wheel Excavator's Boom during the Excavation Process. *Sustainability* **2019**, *11*, 4357. [[CrossRef](#)]
11. Sowała, M.; Strempsi, A.; Woźniak, J.; Pactwa, K. Impact of the Length of Manoeuvring Roads of a Bucket Wheel Excavator for Working Times in the Shortwall. *J. Min. Sci.* **2019**, *55*, 603–609. [[CrossRef](#)]
12. Machniak, L.; Koziol, W. Method of assessment of hard rock workability using bucket wheel excavators. *Arch. Min. Sci.* **2017**, *62*, 73–82. [[CrossRef](#)]
13. Bolukbasi, N.; Koncagul, O.; Pasamehmetoglu, A.G. Material diggability studies for the assessment of bucket wheel excavator performance. *Min. Sci. Technol.* **1991**, *13*, 271–277. [[CrossRef](#)]
14. Chen, Z.; Chen, Y. Determination and analysis of the theoretical production of a bucket wheel excavator. *Arch. Min. Sci.* **2014**, *59*, 283–291.
15. Xiang, Y.; Mutschler, S.; Brix, N.; Brach, C.; Geimer, M. Optimization of Operation Strategy for Primary Torque based Hydrostatic Drivetrain using Artificial Intelligence. *arXiv* **2020**, arXiv:2003.10011.
16. Xiang, Y.; Tang, T.; Su, T.; Brach, C.; Liu, L.; Mao, S.S.; Geimer, M. Fast CRDNN: Towards on Site Training of Mobile Construction Machines. *IEEE Access* **2021**, *9*, 124253–124267. [[CrossRef](#)]
17. Kostić, S.; Trivan, J. Optimization of coal overburden excavation considering variable geomechanical properties and states of excavator teeth. *Arch. Min. Sci.* **2022**, *67*, 123–142.
18. Ignjatović, D. *Study on Optimization of the Construction of Buckets of the Buecket-Wheel Excavator in Order to Increase the Capacity of the Excavator*; University of Belgrade Faculty of Mining and Geology: Belgrade, Serbia, 2003; p. 218. (In Serbian)
19. Bergen, K.J.; Johnson, P.A.; de Hoop, M.V.; Beroza, G.C. Machine learning for data-driven discovery in solid Earth geoscience. *Science* **2019**, *363*, eaau032. [[CrossRef](#)] [[PubMed](#)]
20. Reichstein, M.; Camps-Valls, G.; Stevens, B.; Jung, M.; Denzler, J.; Carvalhais, N.; Prabhat, F. Deep learning and process understanding for data-driven Earth system science. *Nature* **2019**, *566*, 195–204. [[CrossRef](#)] [[PubMed](#)]
21. Mignan, A.; Broccardo, M. Neural network applications in earthquake prediction (1994–2019): Meta-analytic and statistical insights on their limitations. *Seismol. Res. Lett.* **2020**, *91*, 2330–2342. [[CrossRef](#)]
22. LeCun, Y.; Bengio, Y.; Hinton, G. Deep learning. *Nature* **2015**, *521*, 436–444. [[CrossRef](#)] [[PubMed](#)]
23. Glorot, X.; Bengio, Y. Understanding the difficulty of training deep feedforward neural networks. In Proceedings of the Thirteenth International Conference on Artificial Intelligence and Statistics, JMLR Workshop and Conference Proceedings, Sardinia, Italy, 13 May 2010; pp. 249–256.
24. Gal, Y.; Ghahramani, Z. Dropout as a bayesian approximation: Representing model uncertainty in deep learning. In Proceedings of the International Conference on Machine Learning, New York, NY, USA, 19–24 June 2016; pp. 1050–1059.
25. Zeiler, M.D. Adadelta: An adaptive learning rate method. *arXiv* **2012**, arXiv:1212.5701.
26. Kingma, D.P.; Ba, J. Adam: A method for stochastic optimization. *arXiv* **2014**, arXiv:1412.6980.
27. Bottou, L. Large-scale machine learning with stochastic gradient descent. In Proceedings of the COMPSTAT'2010: 19th International Conference on Computational Statistics, Paris, France, 22–27 August 2010; Keynote, Invited and Contributed Papers. pp. 177–186.

**Disclaimer/Publisher's Note:** The statements, opinions and data contained in all publications are solely those of the individual author(s) and contributor(s) and not of MDPI and/or the editor(s). MDPI and/or the editor(s) disclaim responsibility for any injury to people or property resulting from any ideas, methods, instructions or products referred to in the content.